Proceedings of "Applications of Physics in Mechanical and Material Engineering" (APMME 2023)

Magnetic Interactions and Coercivity Mechanism in Nanocrystalline Nd–Fe–B Ribbons with Nb Addition

A. Przybył[a,*], I. Wnuk[a], J. Wysłocki[a], K. Kutynia[a], M. Kaźmierczak[b], M. Rychta[a] and P. Gębara[a]

[a] *Department of Physics, Czestochowa University of Technology, Armii Krajowej 19, 42-200 Częstochowa, Poland*
[b] *Complex of Schlools in Goleniowy, Kościuszki 20, 42-445 Szczekociny, Poland*

Doi: 10.12693/APhysPolA.144.333 *e-mail: anna.przybyl@pcz.pl

In the present paper, the phase structure, magnetic properties, and magnetization reversal processes in the $(Nd_{10}Fe_{67}B_{23})_{93}Nb_7$ alloy ribbon were investigated. The X-ray diffraction analysis revealed a coexistence of the following phases: hard magnetic $Nd_2Fe_{14}B$, metastable soft magnetic $Nd_2Fe_{23}B_3$, and paramagnetic $Nd_{1+\varepsilon}Fe_4B_4$. Moreover, the changes in phase composition were noticed after heat treatment. In order to check magnetic measurements, the hysteresis loops were collected. The magnetization reversal curves were studied by constructing the reversible part of magnetization dependence on the irreversible part of magnetization.

topics: X-ray diffraction (XRD), magnetic properties, magnetization reversal processes

1. Introduction

Although the Nd–Fe–B permanent magnets have been well-known for over forty years, they are still intensively studied. Moreover, magnets of this type, due to their excellent properties and relatively low price, are widely used in the latest technologies [1–4]. The good magnetic properties of the Nd–Fe–B alloys, such as coercivity ${}_JH_C$, remanence B_r, or maximum energy product $(BH)_{max}$, are related to the appropriate structure and phase composition of these alloys. For some time, they have been produced using rapid quenching methods such as suction casting, melt-spinning, or injection casting. Selective modification of chemical composition and specific annealing conditions are required to achieve the best magnetic properties [5]. For many years, the chemical compositions of the Nd–Fe–B-type alloys have been selectively modified in order to change their phase structure and magnetic properties. Among others, the Nb alloying has been intensively studied due to its influence on glass forming ability or reduction of growth of nanocrystalline grains formed during heat treatment [6–9] and, in consequence, modification of magnetic properties. The time and temperature of heat treatment are also extremely important, taking into account the formation of the microstructure and specific phase constitution. These two parameters have significant influence on the coercivity of produced magnets. The mechanisms of coercivity could be better understood by investigation of magnetization reversal processes.

According to that, the structure, magnetic properties, magnetic interactions, and coercivity mechanisms of the $(Nd_{10}Fe_{67}B_{23})_{93}Nb_7$ alloy ribbons.

2. Material and experimental techniques

The ingot sample with nominal composition $(Nd_{10}Fe_{67}B_{23})_{93}Nb_7$ was produced by arc-melting of the high purity (min. 4 N) elements under low pressure of inert gas (Ar). Boron was added in the form of Fe–B alloy with a well-known composition. Ribbons were produced by the melt-spinning technique under low pressure of a protective atmosphere (Ar). Produced ribbons were sealed off in quart tubes under a low pressure of Ar gas and annealed in a wide range of temperatures for 5 min. The X-ray diffraction (XRD) studies were performed using Bruker D8 ADVANCE diffractometer with Cu K_α radiation and LYNXEYE semiconductor detector. Magnetic properties were measured using the Lake Shore 7307 vibrating sample magnetometer working in an external magnetic field up to ~ 2 T.

3. Results and discussion

Fig. 1 shows the X-ray diffraction pattern of the $(Nd_{10}Fe_{67}B_{23})_{93}Nb_7$ alloy ribbon in an as-cast state and after heat treatment at 1003 K for 5 min. The analysis revealed that the sample in an as-cast state is partially amorphous. However, a coexistence of the expected ferromagnetic $Nd_2Fe_{14}B$ phase, paramagnetic $Nd_{1+\varepsilon}Fe_4B_4$ phase, and metastable $Nd_2Fe_{23}B_3$ phase was detected. A significant increase in the content of the $Nd_2Fe_{14}B$ phase at the expense of the amorphous phase was observed after annealing at 1003 K for a relatively short time.

Magnetic hysteresis loops of the $(Nd_{10}Fe_{67}B_{23})_{93}Nb_7$ alloy were collected in Fig. 2. Hysteresis loops of the studied sample in an as-cast state and annealed at 923 K are typical for soft magnetic materials (Fig. 2a). However, a heat treatment at 943 K induces some changes in the shape of hysteresis loops. The shape of the hysteresis loop (at 943 K) is called a wasp-waisted loop [10] and is typical for samples with a small content of ferromagnetic phases in phase constitution and multiphase samples. The minority

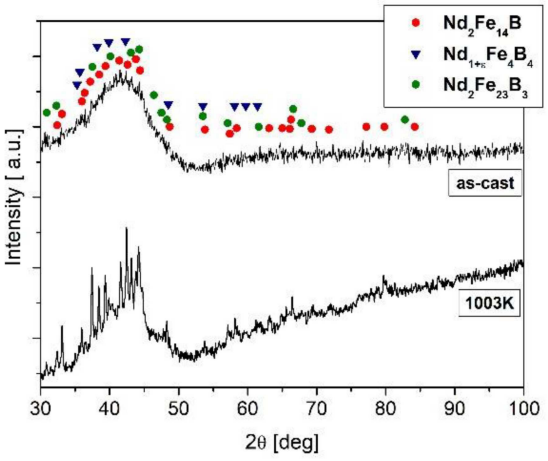

Fig. 1. XRD patterns of the $(Nd_{10}Fe_{67}B_{23})_{93}Nb_7$ alloy ribbon in as-cast state and after heat treatment at 1003 K for 5 min.

TABLE I

Magnetic parameters of the $(Nd_{10}Fe_{67}B_{23})_{93}Nb_7$ alloy ribbon annealed at 963–1063 K with step 20 K for 5 min.

Annealing temperature [K]	J_r [T]	$_JH_C$ [kA/m]	$(BH)_{max}$ [kJ/m^3]
963	0.42	1083	30.7
983	0.44	835	27.1
1003	0.36	924	34.0
1023	0.45	852	30.4
1043	0.51	856	38.6
1063	0.50	702	30.6

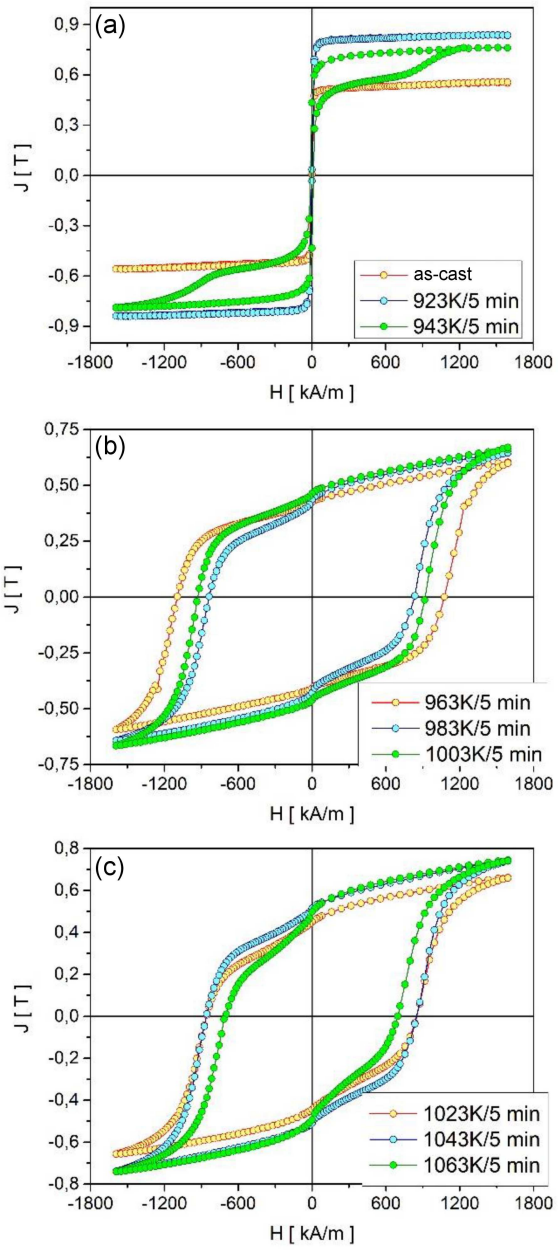

Fig. 2. Magnetic hysteresis loops of the $(Nd_{10}Fe_{67}B_{23})_{93}Nb_7$ alloy ribbon in as-cast state and after heat treatment in the temperature range from 923 to 1063 K for 5 min.

content of the hard magnetic $Nd_2Fe_{14}B$ phase with the majority content of soft magnetic $Nd_2Fe_{23}B_3$ phase and paramagnetic $Nd_{1+\varepsilon}Fe_4B_4$ phase causes a contraction of the hysteresis loop in the vicinity of coercivity. An increase in temperature of heat treatment caused the broadening of hysteresis loops, which resulted in an increase in hard magnetic phase content. Moreover, the shapes of hysteresis loops in the range 963–1063 K are typical for multiphase samples, which was confirmed by the XRD studies. Basic magnetic properties determined from hysteresis loops are summarized in Table I.

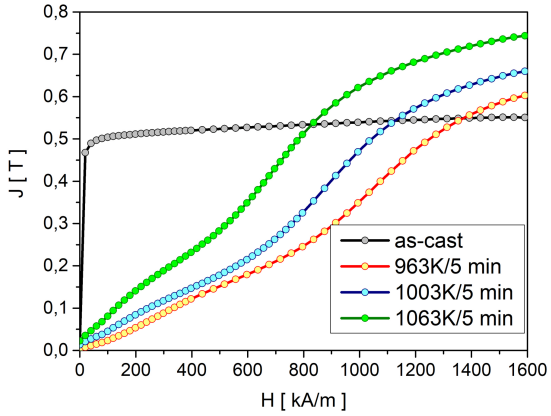

Fig. 3. Magnetization virgin curves of the studied alloy ribbon in the as-cast state and after heat treatment at selected temperatures.

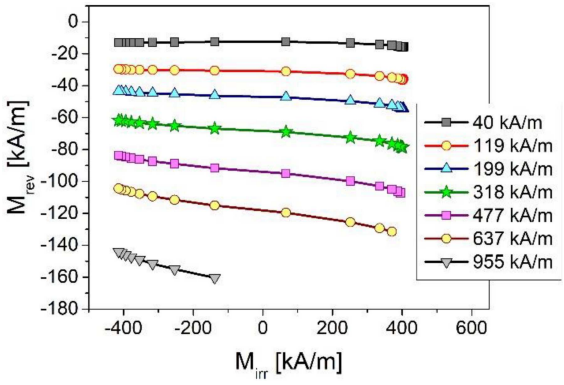

Fig. 4. The M_{rev} vs M_{irr} curves constructed for studied $(Nd_{10}Fe_{67}B_{23})_{93}Nb_7$ alloy ribbon annelaed at 1003 K for 5 min.

Maximum coercivity was revealed for the sample annealed at 963 K. However, the highest remanence and maximum density of magnetic energy were detected for ribbon heated at 1043 K. Magnetization virgin curves for the sample in an as-cast state and for selected annealing temperatures were plotted in Fig. 3. Measurements of the virgin curves were carried out for thermally demagnetized samples. The shape of virgin curve for the sample in an as-cast state is typical for soft magnetic materials. Short time (5 min) annealing at 963 K and higher temperatures induces noticeable changes in the shape of magnetization virgin curves, and a characteristic inflection point was observed. Such behavior is typical for materials in which the magnetization reversal process is based on the pinning of domain walls. Based on them, a further analysis of the magnetization reversal curves was carried out [11–13]. These data were used for the calculation of the dependence of the irreversible part of magnetization on the reversible part of magnetization [14] under the change of several values of an external magnetic field. These curves were collected in Fig. 4.

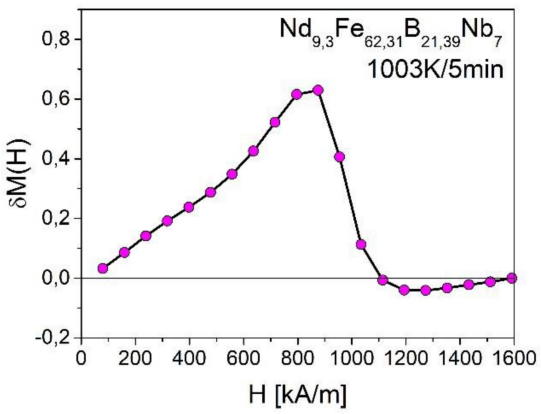

Fig. 5. Henkel plot constructed for studied alloy annealed at 1003 K for 5 min.

A trend of the M_{rev} vs M_{irr} curves is related to the distribution of nucleation fields H_{N} and pinning field H_{P} and the degree of overlapping between these fields [15]. Observed curves were not characterized by any visible minimum. The analysis of the curves indicated that the nucleation process started at stronger magnetic fields, while the pinning field was weaker than the nucleation field. The reversible part of magnetization decreased monotonically, while an increase in the irreversible part of magnetization was observed.

The magnetic interactions between grains in the investigated alloy were studied by the construction of $\delta M(H)$ dependence, called the Henkel plot (see Fig. 5).

The XRD studies confirmed the coexistence of the $Nd_2Fe_{14}B$ and $Nd_2Fe_{23}B_3$ phases. An occurrence of these two phases induces interactions between them. A sharp increase in the range of field 0–800 kA/m in the $\delta M(H)$ curve suggests the strengthening of exchange interactions between grains of these two phases. Positive values of the Henkel plot are caused by strong exchange interactions between soft and hard magnetic phases, while the negative ones are related to weak dipole interactions lowering the magnetization. The observed maximum of the Henkel plot is related to the energy of the interactions.

4. Conclusions

In the present studies, the magnetic properties, magnetization reversal processes, and magnetic interactions were investigated. The XRD measurements revealed the coexistence of the hard ($Nd_2Fe_{14}B$) and soft ($Nd_2Fe_{23}B_3$) magnetic phases. The ribbon in an as-cast state was soft magnetic, however, annealing induced changes in the phase constitution, which caused an improvement in magnetic properties. The analysis of magnetic reversal processes revealed the pinning mechanism as a dominant in produced material.

Acknowledgments

The Authors would like to thank Professor Jan Świerczek, Head of Department of Physics, Częstochowa University of Technology, for financial support.

References

[1] A. Manaf, R.A. Buckley, H.A. Davies, M. Leonowicz, *J. Magn. Magn. Mater.* **101**, 360 (1993).

[2] A. Przybył, *Acta Phys. Pol. A* **135**, 288 (2019).

[3] R. Tamura, S. Kobayashi, T. Fukuzaki, M. Isobe, Y. Ueda, *J. Phys. Conf. Ser.* **144**, 012068 (2009).

[4] M. Szwaja, P. Pawlik, J.J. Wysłocki, P. Gębara, *Archiv. Mettal. Mater.* **57**, 233 (2012).

[5] A. Przybył, K. Pawlik, P. Pawlik, P. Gębara, J.J. Wysłocki, *J. Alloys Compd.* **536S**, 333 (2012).

[6] H.R. Kirchmayr, *J. Phys. D Appl. Phys.* **29**, 2763 (1996).

[7] J. Zhang, K.Y. Lim, Y.P. Feng, Y. Li, *Scr. Mater.* **56**, 943 (2007).

[8] I. Wnuk, A. Przybył, M. Kaźmierczak, *Acta Phys. Pol. A* **138**, 166 (2020).

[9] A. Przybył, *Acta Phys. Pol. A* **138**, 144 (2020).

[10] I. Wnuk, A. Przybył, K. Kutynia, J.J. Wysłocki, *Acta Phys. Pol. A* **135**, 292 (2019).

[11] D.C. Crew, L.H. Lewis, D.O. Welch, *J. Appl. Phys.* **87**, 4744 (2000).

[12] D.C. Crew, K.H. Lewis, *J. Appl. Phys.* **87**, 4783 (2000).

[13] H. Zhang, Ch. Rong, X. Du, J. Zhang, S. Zhang, B. Shen, *Appl. Phys. Lett.* **82**, 4098 (2003).

[14] M. Szwaja, K. Pawlik, P. Pawlik, P. Gębara, B. Michalski, *Acta Phys. Pol. A* **127**, 623 (2015).

[15] P.E. Kelly, K. O'Grady, P.I. Mayo, R.W. Chantrell, *IEEE Trans. Magn.* **25**, 3881 (1989).